HOSTED BY
ELSEVIER
CrossMark
Available online at www.sciencedirect.com
ScienceDirect
Karbala International Journal of Modern Science 1 (2015) 142–151
http://www.journals.elsevier.com/karbala-international-journal-of-modern-science/

Electronic and structural properties of nitrogen-vacancy center in diamond nanocrystals: A theoretical study

Mudar A. Abdulsattar

Ministry of Science and Technology, Baghdad, Iraq

Received 3 July 2015; revised 3 October 2015; accepted 28 October 2015
Available online 8 December 2015

Abstract

Neutral and negatively charged nitrogen-vacancy centers in hydrogenated diamond nanocrystals are investigated including singlet and triplet spin states. The investigation is carried out using density functional theory at the generalized gradient approximation level of Perdew–Burke–Ernzerhof. Dilation and distortion in the direction of the N-Vacancy direction is observed. The smallest gap and the highest number of energy levels that enter the original unaltered forbidden energy gap are in the triplet state of the negatively charged nitrogen-vacancy center. Results show that the dipole moment and valance band width of the negatively charged nitrogen-vacancy center in the singlet state are the highest between investigated structures. Triplet state has the highest spin density at two carbon atoms near the nitrogen-vacancy with the remaining spin density at the nitrogen atom itself. For the neutral nitrogen-vacancy center the spin density nearly accumulates at one carbon atom near the nitrogen-vacancy only. Analysis of bonds and tetrahedral angles show that the present nitrogen-vacancy centers deviate appreciably from the ordinary structure of unaltered diamond nanocrystals.

Keywords: Nanocrystals; Ab initio calculations; Nitrogen-vacancy

1. Introduction

Nitrogen-vacancy (NV) center in diamond is widely explored in last years. The importance of this defect rises from the possibility of using this center in quantum computing, spintronics and quantum cryptography [1]. This center had been explored experimentally and theoretically in bulk and diamond nanocrystals [1–12]. The exploration of nanoscale properties of this defect is certainly an important step in view of the present direction of reduction in size of different electronics hardware.

NV centers are known from decades, however, its electronic structure is only recently investigated in details [1,2]. The investigation and comparison of some quantities in diamond nanocrystals that contains NV centers can be profitable to understand the way to manipulate these centers using magnetic fields, electric fields or any kind of radiation that interact with the NV center. Such properties that will be investigated in the present work are the energy gap, density of states, dipole moment … etc.

E-mail address: mudarahmed3@yahoo.com.
Peer review under responsibility of University of Kerbala.

http://dx.doi.org/10.1016/j.kijoms.2015.10.008

2. Theory

The unaltered diamond nanocrystal that we chose to insert an NV center in it has the stoichiometry $C_{64}H_{84}$. In choosing the present nanocrystal size, we made sure that the NV center can be inserted away from the surface by three layers. This choice confirms that the NV center is outside the surface reconstruction layers of the nanocrystal [13,14]. The second criterion is that this nanocrystal and its other derived structures are computationally feasible using ab initio methods. NV centers that are analyzed in the present work include the $C_{62}NH_{84}^{(-)}$ (negatively charged diamond nanocrystal that include an NV center in the singlet and triplet states (Fig. 1)) and $C_{62}NH_{84}^{(0)}$ (neutral diamond nanocrystal that include an NV center in the singlet state).

Density functional theory at the generalized gradient approximation of Perdew, Burke and Ernzerhof (PBE) is used to simulate the electronic structure of the various NV center structures. Unrestricted PBE theory is used to simulate odd number of electrons while restricted PBE theory is used to the even number of electrons. Double-zeta 3-21G basis functions are found adequate as a reasonable compromise in terms of computer time and results accuracy. For restricted Fock Hamiltonian (**F**) calculations, only one equation is needed:

$$\mathbf{FC} = \mathbf{SC}\boldsymbol{\varepsilon}, \tag{1}$$

where **C** is the matrix of coefficients, **S** is the overlap integral and ε is the diagonal energy matrix. For the unrestricted Fock theory two equations are needed:

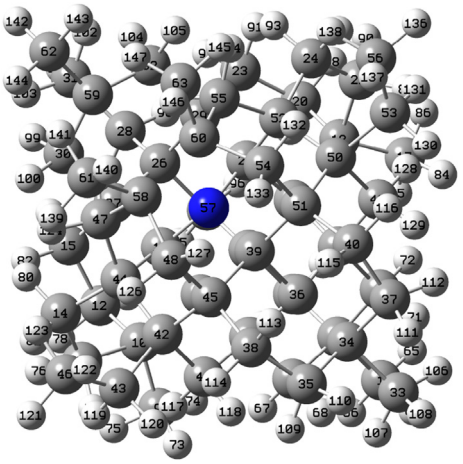

Fig. 1. Diamond nanocrystal with NV^- center in the singlet state. Blue (dark) ball is the nitrogen atom; small white balls are hydrogen atoms. The remaining balls are carbon atoms. Note that the vacancy is at the upper-left side of the nitrogen atom.

$$\mathbf{F}^{\alpha}\mathbf{C}^{\alpha} = \mathbf{S}\mathbf{C}^{\alpha}\boldsymbol{\varepsilon}^{\alpha}, \tag{2}$$

$$\mathbf{F}^{\beta}\mathbf{C}^{\beta} = \mathbf{S}\mathbf{C}^{\beta}\boldsymbol{\varepsilon}^{\beta}, \tag{3}$$

where α and β represents electrons with spin up and spin down respectively.

As a benchmark, the present theory (PBE/3-21G) predicts an energy gap of 7.954 eV for adamantane ($C_{10}H_{16}$) [15] compared with 6.03 eV for the experimental value [16]. Although the present method has 32% error in the value of the energy gap for adamantine, it is still a good compromise between computational efforts and accuracy for size and number of particles (147–148 atoms) in the presently investigated nanocrystal. The value of the gap using B3LYP hybrid functional is 9.8 eV [15]. This explains why we preferred the PBE theory.

CH_3 vibrations are found in experimental infrared spectrum on diamond nanocrystals surfaces [17]. As a result we included some surface CH_3 in the present nanocrystals. Note that CH_3 can be found only at nanocrystals surface corners and not on flat surfaces. Gaussian03 program [18] is used in the present work for all the investigated nanocrystals.

3. Calculations and results

In Figs. 2–4 density of states are collected in intervals of 0.01 Hartrees (0.27211 eV). In the same way in Figs. 5 and 6 bond lengths and tetrahedral angles are collected in 0.01 Å and 1° intervals respectively. The energy gaps are identified as to be between the HOMO and LUMO levels.

Fig. 2 shows a comparison between density of states of an ideal diamond nanocrystal, and singlet state of a diamond nanocrystal with NV^- center. Fig. 3 shows a comparison between density of states of α and β electrons in diamond nanocrystal with NV^0 center. Fig. 4 on the other hand shows density of states of α and β electrons in triplet state of diamond nanocrystal with NV^- center. Unlike Fig. 2 states can be only singly occupied in Figs. 3 and 4.

Figs. 5 and 6 show the distribution of bond lengths and tetrahedral angle values in unaltered diamond nanocrystal and in diamond nanocrystal with singlet state NV^- center. Finally Fig. 7 shows the position of energy gap location in electronic spectrum of the above investigated states.

Table 1 shows some properties of unaltered diamond nanocrystal and diamond nanocrystals with presently investigated NV centers. These properties include HOMO, LUMO, valance band width (VBW)

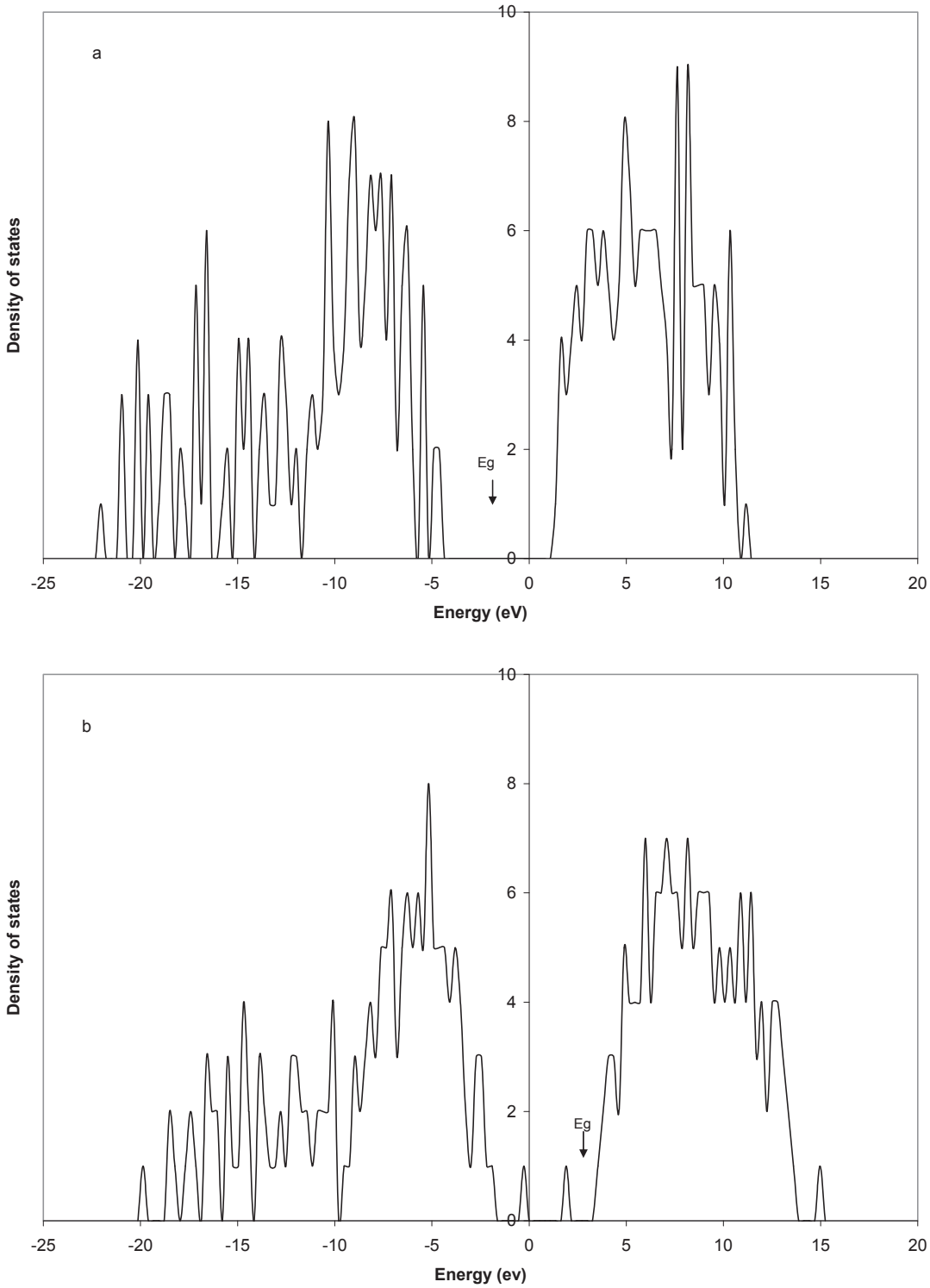

Fig. 2. (a) Density of states of an ideal diamond nanocrystal, and (b) singlet state of a diamond nanocrystal with NV^- center. States can be only doubly occupied in the present figure.

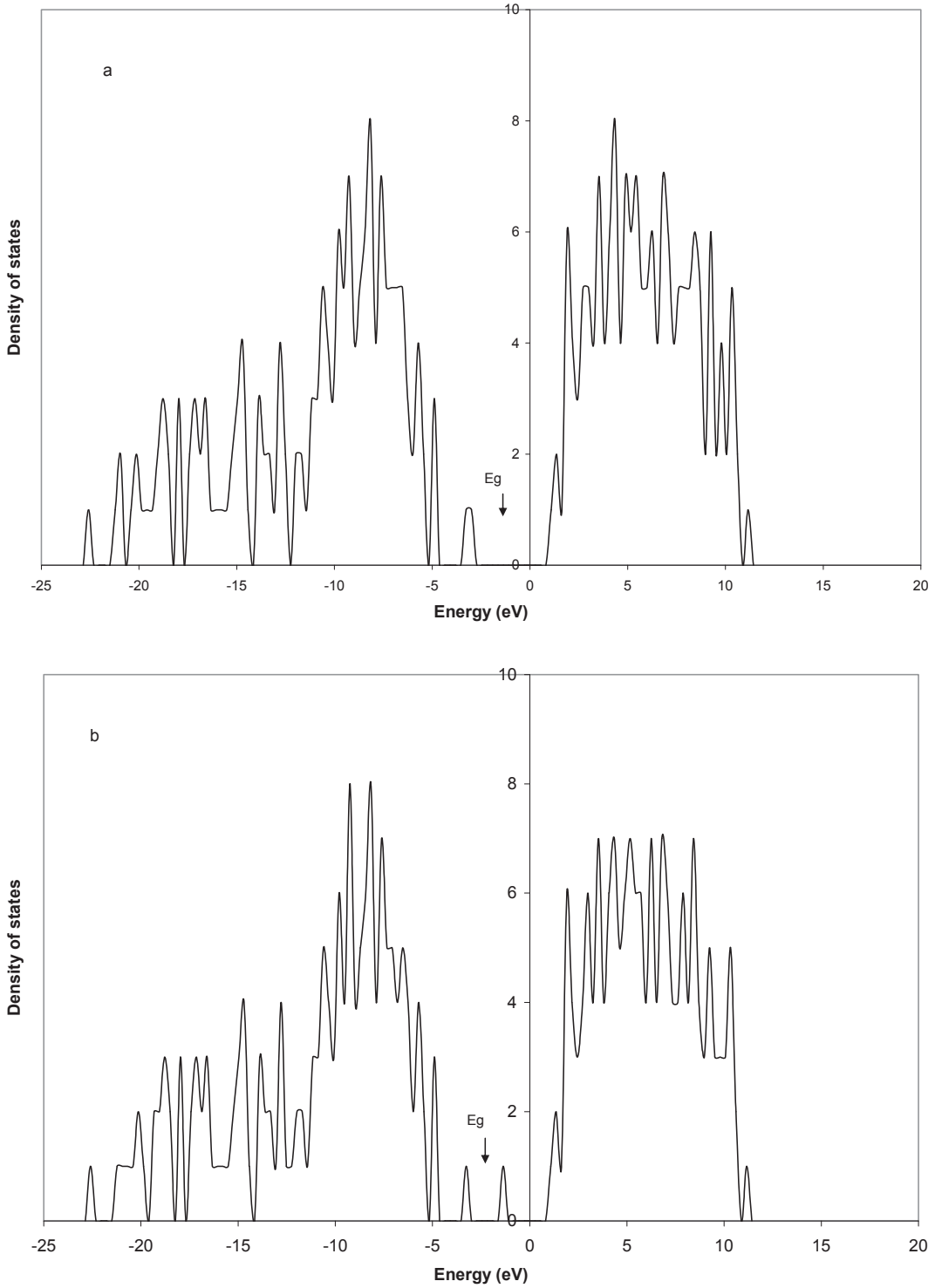

Fig. 3. (a) Density of states of α electrons in diamond nanocrystal with NV^0 center, and (b) β electrons in diamond nanocrystal with NV^0 center. States can be only singly occupied in the present figure.

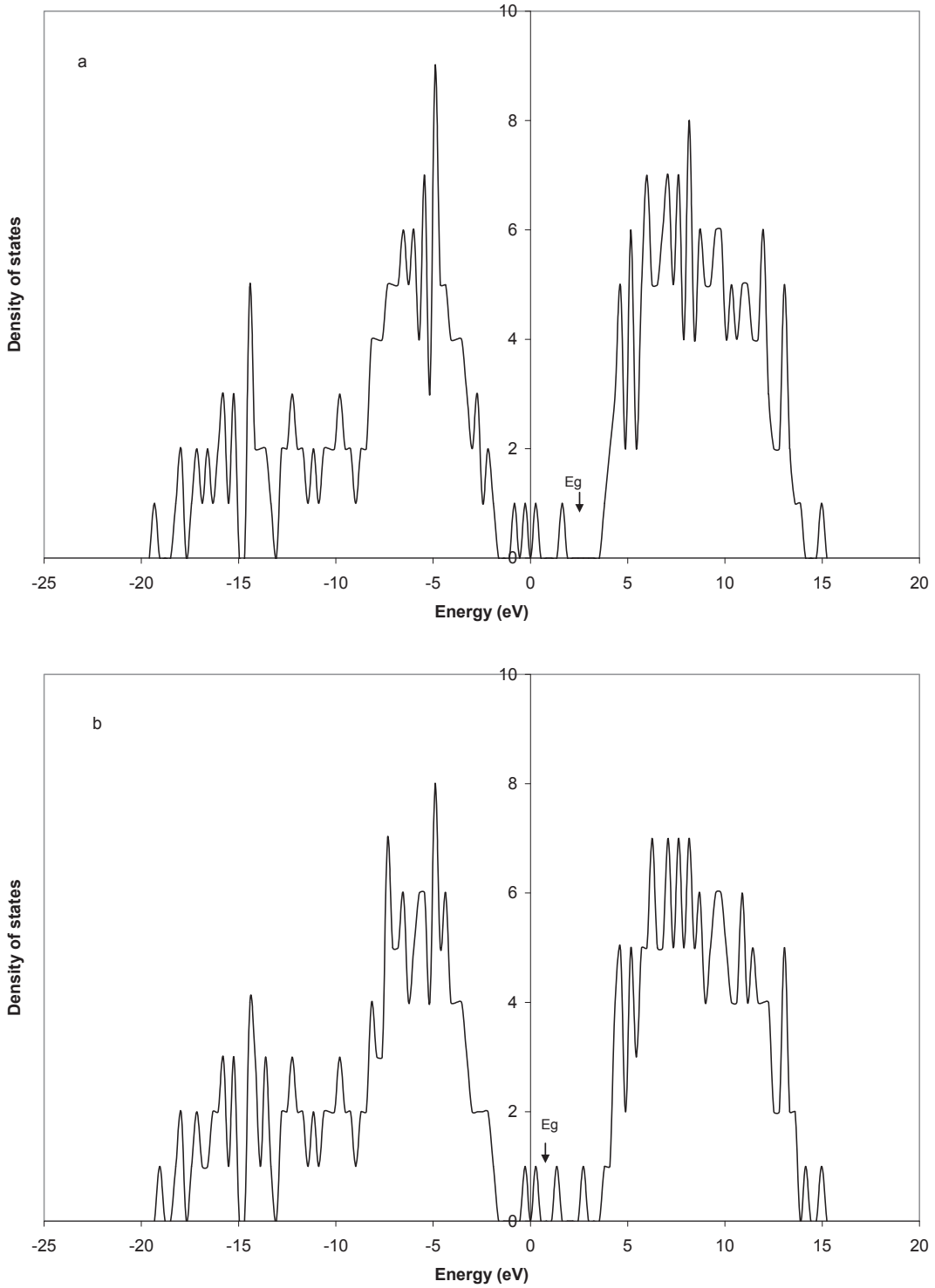

Fig. 4. (a) Density of triplet states of α electrons in diamond nanocrystal with NV^- center, and (b) β electrons in triplet state of diamond nanocrystal with NV^- center. States can be only singly occupied in the present figure.

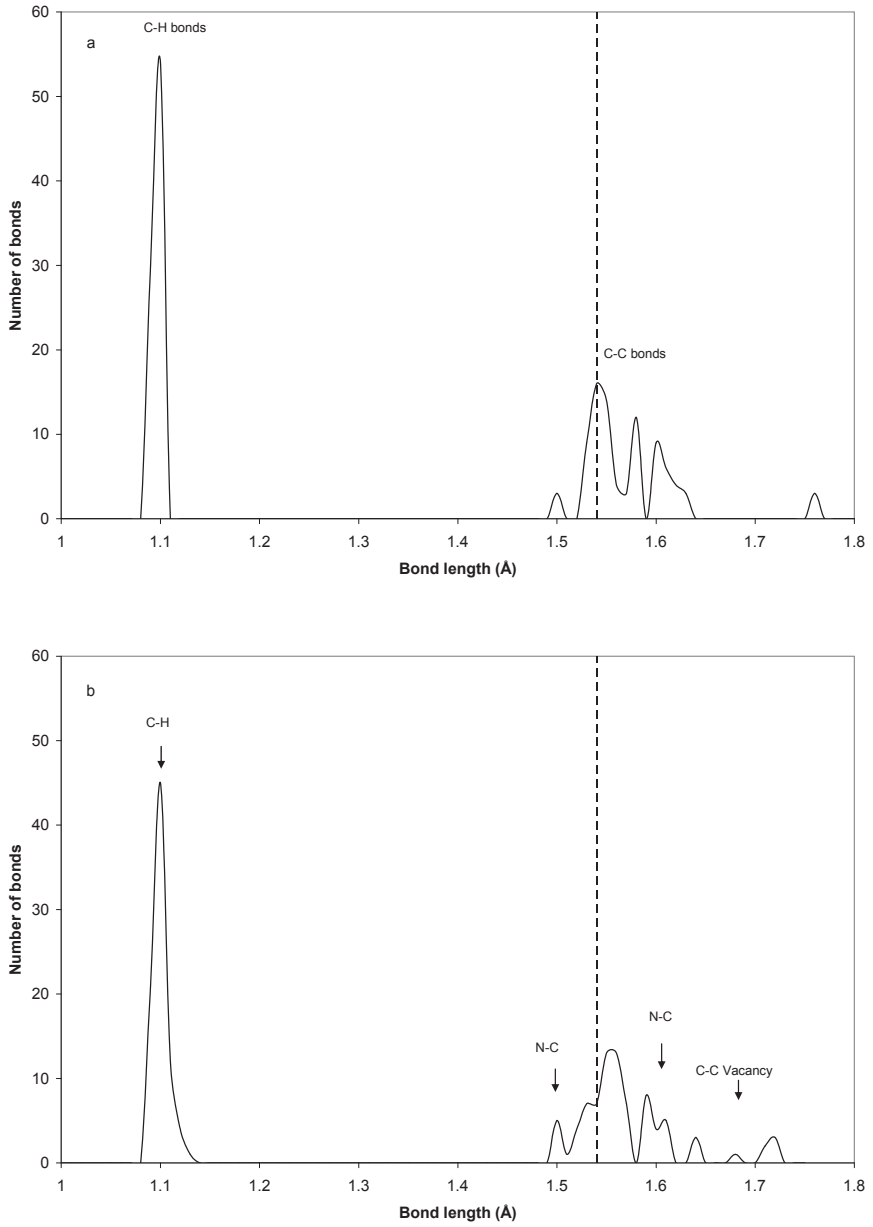

Fig. 5. Distribution of bond lengths in ordinary diamond nanocrystal (a), and bond lengths in diamond nanocrystal with singlet state NV^- center (b). A broken line indicates the value of this bond (1.54 Å) in experimental bulk diamond structure.

and dipole moment. The dipole moment is calculated as function of electronic density (ρ) using the formula:

$$\mathbf{P}(\mathbf{r}) = \int_V \rho(\mathbf{r})\mathbf{r}d^3\mathrm{r}. \quad (4)$$

The dipole moment importance can be appreciated from the fact that it can control the amount of level splitting induced by external electric fields (**E**) as in the stark Hamiltonian [7]:

$$H_{stark} = -\mathbf{p}(\mathbf{r})\cdot\mathbf{E}(\mathbf{r}). \quad (5)$$

4. Discussion and conclusions

Dilation in the direction of the left-top corner is obvious in Fig. 1. This direction is the Nitrogen-Vacancy direction. Heavy reconstruction is also obvious in comparison with the opposite direction (bottom-right direction). This reconstruction can be

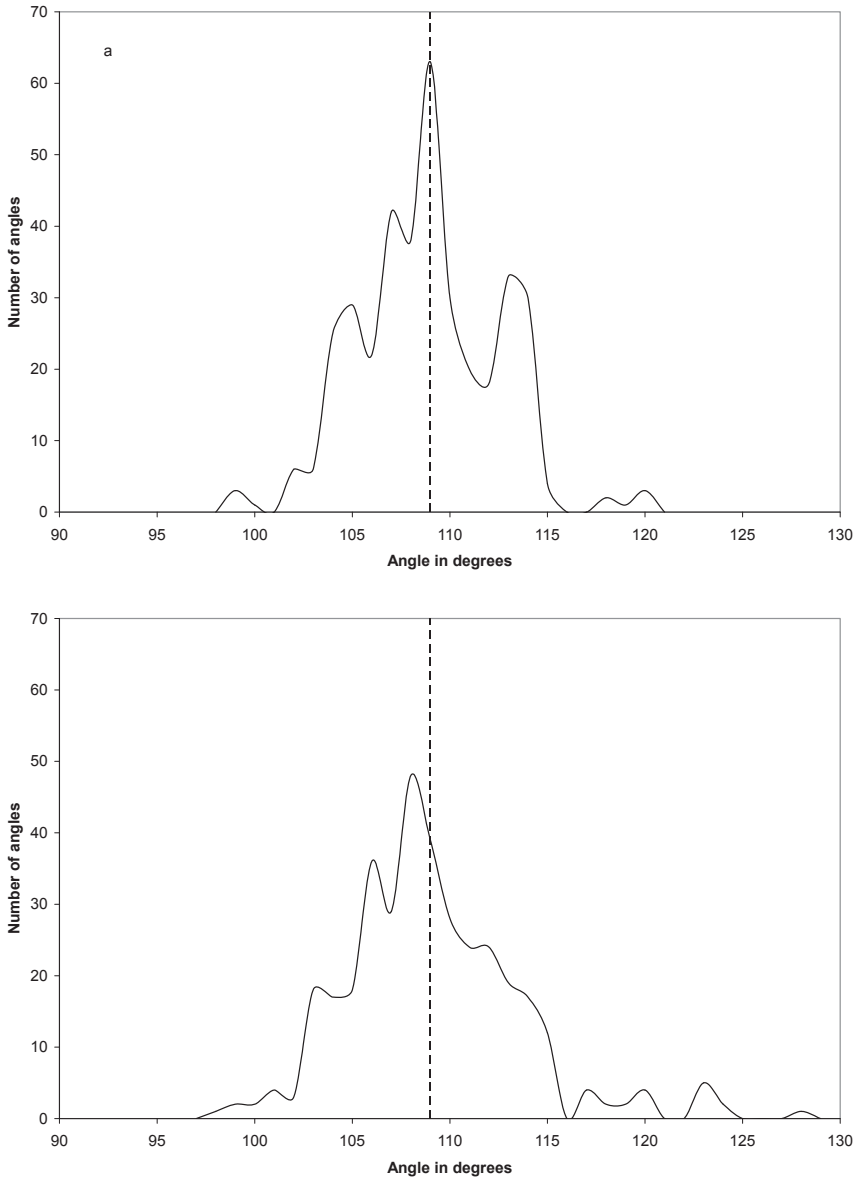

Fig. 6. (a) Distribution of tetrahedral angle values in ordinary diamond nanocrystal, and (b) tetrahedral angel in diamond nanocrystal with NV^- center in the singlet state. A broken line indicates the value of this angle near the ideal diamond structure at (109.47°).

identified by comparing this area with the nearly perfect squares at the middle of the nanocrystal. The distortion of this part of the nanocrystal that accompanies the NV center creation is also noticed in bulk diamond bond lengths and structures [1].

In Fig. 2 we can note several differences between the two parts of the figure. First, area under the curve in Fig. 2a is slightly greater than that in Fig. 2b due to the difference in the number of atoms. Second, the high and sharp peaks in Fig. 2a melt down to fill the inter-distances between these peaks in Fig. 2b. Third, the whole density of states of Fig. 2b is moved toward the positive region due to the extra negative charge in NV^- center. Fourth, in Fig. 2b two levels interred the originally forbidden gap of Fig. 2a which are due to nitrogen impurity and vacancy in NV^- center. Finally, Energy gap of the NV^- center in the singlet state is just 1.75 eV in comparison with 6.23 eV of the unaltered diamond nanocrystal. Although the singlet states have not yet been directly measured in experiments it plays an important role in the emission processes [1].

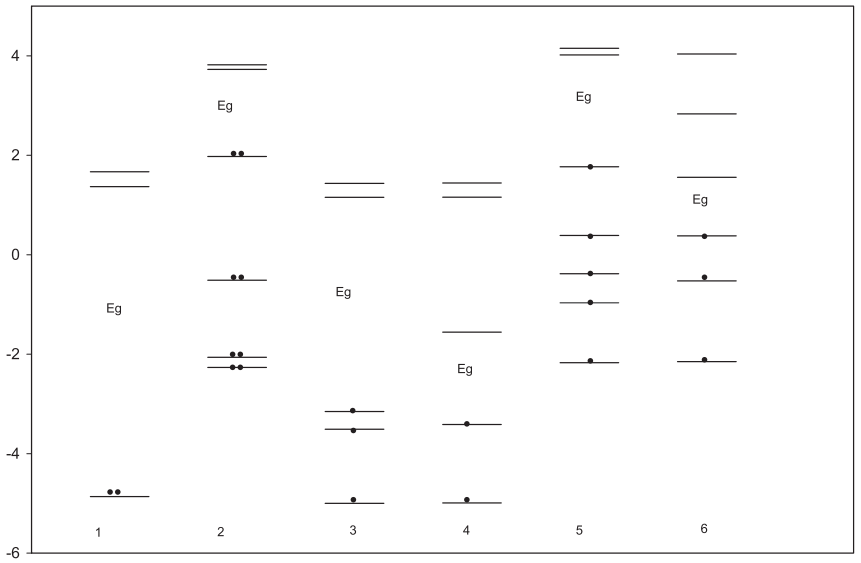

Fig. 7. Energy gap location in electronic spectra of 1- unaltered diamond nanocrystal, 2- singlet state of a negatively charged NV center in diamond nanocrystal, 3 and 4- α and β electrons respectively of neutral NV center, 5 and 6- α and β electrons respectively of the triplet state of a negatively charged NV center in diamond nanocrystal.

Table 1
Some properties of ordinary diamond nanocrystal ($C_{64}H_{84}$) and diamond nanocrystals with various investigated NV centers (the remaining columns).

	$C_{64}H_{84}$	$C_{62}NH_{84}^{(-)}$ (singlet)	$C_{62}NH_{84}^{(0)}$		$C_{62}NH_{84}^{(-)}$ (triplet)	
			α	β	α	β
HOMO (eV)	−4.864	1.976	−3.154	−3.414	1.771	0.380
LUMO (eV)	1.371	3.729	1.155	−1.555	4.017	1.556
VBW (eV)	17.277	22.023	19.621	19.357	21.129	19.644
Dipole moment (Debye)	0.0375	9.3414	1.1899		2.670	

Fig. 3 shows density of state of α electrons (spin up) and β electrons (spin down) in diamond nanocrystal with NV^0 center. α electrons are greater than β electrons by one electron (odd number of electrons) so that the neutral NV center is paramagnetic [13]. β electrons differ from α electrons by the existence of an empty level at −1.555 eV (this is also obvious in Fig. 7 column 4 and Table 1). The extra electron in the α electrons affects the density of states by bringing closer the −1.555 eV level to the already existing level at −3.4 eV. The neutral NV center was proposed as a qubit in addition to the negatively charged NV center in the triplet state [10].

Fig. 4 shows the density of triplet states of α and β electrons in diamond nanocrystal with NV^- center. This figure shows that the triplet state has more states in originally forbidden gap of Fig. 2a. In fact, the triplet state has more states in this gap than all other investigated examples in the present work. This state is investigated both experimentally and theoretically. The energy gap for α electrons in this state is 2.246 eV. The experimental analog of this gap of NV^-centers in bulk diamond is 1.945 eV. Considering error estimates of the present method presented in the theory part, it is not clear whether this increase of the gap is due to quantum confinement effects or calculation errors at the present theory level. In all cases, other calculations of this gap in bulk diamond ranges from 1.71 to 1.77 eV using different methods [1].

Distribution of bond lengths in ordinary diamond nanocrystal and bond lengths in diamond nanocrystal NV^- center at singlet state are shown in Fig. 5. A broken line indicates the value of C–C experimental bond (1.54 Å) in bulk diamond structure. As we can note from this figure that bond lengths is in general agreement with bond lengths found in ordinary

reconstructed diamond surfaces [14]. However, we must keep in mind that we are considering diamond nanocrystal that differs from reconstructed bulk diamond flat surfaces by the fact that diamond nanocrystals surfaces are rounded and might have edges and corners. This explains the occurrence of CH_3 on diamond nanocrystals surfaces and not in bulk diamond flat surfaces [14]. The effect of NV^- center on bond lengths is obvious that include the new N–C bonds and the effect of vacancy and its dangling bonds. The highest peak is the C–H bond peak which is around 1.1 Å in agreement with experiment. However, these bonds are less sharp and have a tail towards higher values in a diamond nanocrystal with an NV^- center as in Fig. 5a. The same is true for the C–C bonds.

Distribution of tetrahedral angle values in ordinary diamond nanocrystal, and diamond nanocrystal with NV^- center in the singlet state is shown in Fig. 6. A broken line indicates the value of this angle near the ideal diamond structure at 109.47°. We can note from this figure that the highest peak for the unaltered diamond nanocrystal (Fig. 6a) is at the ideal diamond structure. The shape of the distribution is like an asymmetric diffraction pattern. In general, the angles that are closer to the middle of the nanocrystal are closer to the ideal value of 109.47°. The insertion of an NV^- center partially destroys the nanocrystal tetrahedral angel distribution with the highest peak is at 108°. As in the previous figures, the angles in diamond nanocrystal with an NV^- center (Fig. 6b) seems to be as a melt down of the figure of the ideal nanocrystal (Fig. 6a).

Fig. 7 allocates the energy gaps in the various electronic spectra of the present work. We can note from this figure and the previous figures (Figs. 2–4) that the original energy gap is approximately the same with the exclusion of the new states that entered this gap due to the NV center. However, this gap rises relatively in negatively charged nanocrystals due to electron–electron interaction as can be seen in columns 2, 5 and 6 in Fig. 7.

Table 1 shows the values of HOMO and LUMO levels for the investigated nanocrystals. The energy gaps that are obtained from these levels as in Table 1 are 6.23, 1.75, 4.31, 1.86, 2.246, and 1.18 eV respectively.

The VBW is a measure of the amount of reconstruction that affects the nanocrystal since reconstruction splits closely degenerate states. Using this criterion, the least reconstruction is in the unaltered nanocrystal. The heaviest reconstruction is in the singlet NV^- center nanocrystal. This also can be noted from the values of the dipole moment that have its highest value for the singlet NV^- center. For bulk diamond the energy gap and VBW are 5.47 and 21 eV respectively [16,19]. These values compare well with the gaps and VBWs in the present work. The dipole moment of an ideal bulk diamond is nearly zero Debye. This is a consequence of the covalent bonding between carbon atoms. The small dipole moment of unaltered diamond nanocrystal is due to the difference in affinity between surface hydrogen and carbon atoms. The inclusion of a neutral NV center in diamond nanocrystal increases the dipole moment of the diamond nanocrystal more than 30 times. This dipole moment is due to the transfer of an electron from the nitrogen atom to the vacancy region. This dipole moment is greatly enhanced in the negatively charged NV center due to the settlement of the additional electron in the vacancy region.

Spin distribution is previously investigated for NV centers in bulk diamond and nanocrystals [1–6]. Only the singlet NV^0 and triplet NV^- states have spin distribution in the present work since they were calculated using unrestricted DFT method. Triplet state in the present nanocrystal has the highest spin density at two carbon atoms (atoms numbered 59 and 39 in Fig. 1) near the NV center with the remaining spin density at the nitrogen atom itself (atom number 57 in Fig. 1). Not that the three atoms are nearly at one line and the vacancy is between atom 59 and nitrogen atom. For the neutral nitrogen-vacancy center the spin density nearly accumulates at one carbon atom only near the vacancy (atom numbered 59 in Fig. 1).

As concluding remarks, we can observe that the smallest gap and the highest number of energy levels that enter the original forbidden energy gap are in the triplet state of the negatively charged nitrogen-vacancy center. The dipole moment and valance band width of the negatively charged nitrogen-vacancy center in the singlet state are the highest between investigated structures. Triplet state has the highest spin density at two carbon atoms near the nitrogen-vacancy with the remaining spin density at the nitrogen atom itself. For the neutral nitrogen-vacancy center the spin density nearly accumulates at one carbon atom only. Bonds at a nanocrystal that contains a nitrogen-vacancy center are generally slightly higher than the same bonds at the unaltered nanocrystal. Tetrahedral angles have the opposite situation in which nanocrystal that contains a nitrogen-vacancy center has generally slightly lower angles than the nearly ideal angles at the unaltered nanocrystal.

References

[1] A. Gali, M. Fyta, E. Kaxiras, Phys. Rev. B 77 (2008) 155206.
[2] J.A. Larsson, P. Delaney, Phys. Rev. B 77 (2008) 165201.
[3] A. Ranjbar, M. Babamoradi, M. Heidari Saani, M.A. Vesaghi, K. Esfarjani, Y. Kawazoe, Phys. Rev. B 84 (2011) 165212.
[4] A. Laraoui, C.A. Meriles, Phys. Rev. B 84 (2011) 161403.
[5] N.D. Lai, D. Zheng, F. Jelezko, F. Treussart, J. Roch, Appl. Phys. Lett. 95 (2009) 133101.
[6] V.M. Acosta, E. Bauch, A. Jarmola, L.J. Zipp, M.P. Ledbetter, D. Budker, Appl. Phys. Lett. 97 (2010) 174104.
[7] V.M. Acosta, C. Santori, A. Faraon, Z. Huang, K.-M.C. Fu, A. Stacey, D.A. Simpson, K. Ganesan, S. Tomljenovic-Hanic, A.D. Greentree, S. Prawer, R.G. Beausoleil, Phys. Rev. Lett. 108 (2012) 206401.
[8] X.-D. Chen, C.-H. Dong, F.-W. Sun, C.-L. Zou, J.-M. Cui, Z.-F. Han, G.-C. Guo, Appl. Phys. Lett. 99 (2011) 161903.
[9] J. Zhang, C.Z. Wang, Z.Z. Zhu, V.V. Dobrovitski, Phys. Rev. B 84 (2011) 035211.
[10] A. Gali, Phys. Rev. B 79 (2009) 235210.
[11] Y. Shen, T.M. Sweeney, H. Wang, Phys. Rev. B 77 (2008) 033201.
[12] Y. Dai, D. Dai, C. Yan, B. Huang, S. Han, Phys. Rev. B 71 (2005) 075421.
[13] C. Kittel, Introduction to Solid State Physics, seventh ed., Wiley, 1996.
[14] S.J. Sque, R. Jones, P.R. Briddon, Phys. Rev. B 73 (2006) 085313.
[15] release 15b, NIST Computational Chemistry Comparison and Benchmark Database, 2011. see, http://cccbdb.nist.gov/.
[16] T.M. Willey, C. Bostedt, T. van Buuren, J.E. Dahl, S.G. Liu, R.M.K. Carlson, R.W. Meulenberg, E.J. Nelson, L.J. Terminello, Phys. Rev. B 74 (2006) 205432.
[17] C. Wen, Z.H. Jin, X.X. Liu, X. Li, J.Q. Guan, D.Y. Sun, Y.R. Lin, S.Y. Tang, G. Zhou, J.D. Lin, Spectrosc. Spetral Anal. 5 (2005) 681.
[18] M.J. Frisch, et al., Gaussian 03, Revision B.01, Gaussian, Inc., Pittsburgh PA, 2003.
[19] Mudar A. Abdulsattar, Khalil H. Al-Bayati, Phys. Rev. B 75 (2007) 245201.